

PCCP

Accepted Manuscript



This is an *Accepted Manuscript*, which has been through the Royal Society of Chemistry peer review process and has been accepted for publication.

Accepted Manuscripts are published online shortly after acceptance, before technical editing, formatting and proof reading. Using this free service, authors can make their results available to the community, in citable form, before we publish the edited article. We will replace this *Accepted Manuscript* with the edited and formatted *Advance Article* as soon as it is available.

You can find more information about *Accepted Manuscripts* in the [Information for Authors](#).

Please note that technical editing may introduce minor changes to the text and/or graphics, which may alter content. The journal's standard [Terms & Conditions](#) and the [Ethical guidelines](#) still apply. In no event shall the Royal Society of Chemistry be held responsible for any errors or omissions in this *Accepted Manuscript* or any consequences arising from the use of any information it contains.

**Density-functional Calculations of the Conversion of
Methane to Methanol on Platinum-decorated Sheets of
Graphene Oxide**

Shiuan-Yau Wu, Chien-Hao Lin and Jia-Jen Ho *

Department of Chemistry, National Taiwan Normal University

No. 88, Section 4, Tingchow Road, Taipei 116, Taiwan

Corresponding author E-mail: jjh@ntnu.edu.tw

Phone: (886)-2-77346223

Fax: (886)-2-29324249

Abstract

By means of calculations based on density-functional theory (DFT), we have investigated the conversion of methane on two platinum atoms supported with a graphene-oxide sheet (Pt₂/GO). In our calculations, a CH₄ molecule can be adsorbed around the Pt atoms of the Pt₂/GO sheet with adsorption energies within -0.11 ~ -0.53 eV; an elongated C-H bond indicates that Pt atoms on that sheet can activate the C-H bond of a CH₄ molecule. The role of the GO sheet in the activation of CH₄ was identified according to an analysis of the electronic density: the GO sheet induces the d-band of Pt atoms to generate several specific d_{z²} state features above the Fermi level, which enabled activation of the C-H bond of CH₄ on generating an evident area of overlap with the hydrogen s orbital of the C-H bond. Upon a dioxygen molecule being added onto the Pt₂/GO sheet, this molecule can react with activated CH₄ according to mechanisms of form $2 \text{CH}_4 + \text{O}_2 \xrightarrow{[\text{Pt}_2/\text{GO}]} 2 \text{CH}_3\text{OH}$, and restore the original Pt₂/GO sheet.

1. Introduction

The development of alternative energy resources is one of the most important issues in the world and has been studied extensively. Among the various work, it is claimed that the preparation of methanol becomes an important role of industry.¹⁻⁵ As methane is an abundant and readily accessible natural resource, a catalytic conversion of methane to methanol or other hydrocarbon or oxide becomes a prominent issue, either experimentally or theoretically,⁶⁻⁹ where the breaking of high C-H bond strength of methane is the first step to convert methane into methanol and it can be activated by the catalysts (metal cluster with very high reactivity in microporous structure, or metal oxide catalysts), followed by the formation of methyl radicals to produce oxygenated products (the controlled oxidation reaction is complicated by the surroundings of enzymatic system). According to these reports, the platinum atoms might increase the adsorption energies of hydrocarbon species, and facilitate scission of the C-H bond. The specific activity of a catalyst is related to the particle size and dispersion; highly distributed metallic particles of small size on supports are generally considered to be ideal catalytic materials.¹⁰ A selection of suitable supports that might yield smaller particles and enhance their dispersion has hence become an important aspect of heterogeneous catalytic reactions.

Graphene oxide (GO) is an attractive option for a suitable support regarding the

dispersion of Pt particles and an improved control of size, because of the active oxygen atoms on the sheet;¹¹ this material has been well applied in fuel cells, sensors and gas storage and catalysts.¹²⁻¹⁴ In addition, the oxygen groups¹⁵ and defect sites¹⁶ of graphene oxide would induce the variation of the d-band structure of supported Pt on Pt/GO sheets, which might enhance the catalytic activity and the tolerance to CO poisoning, relative to commercial carbon-supported Pt catalysts (Pt/C).¹⁴ Although there are many models to simulate GO sheets¹³⁻¹⁸, the common ground of these models is the content of functional groups of two types including epoxy (O) and hydroxyl (OH) with varied O/C ratios. Infrared spectra confirmed that the two most obvious intense absorption lines of a GO sheet are associated with the O-H stretching and C-O (epoxy) stretching modes, at 3458 and 1116 cm^{-1} respectively; the intensity of the C-O (epoxy) line is observed to be much greater than that of the O-H signal¹³. Incidentally, although there is a theoretical calculation¹⁸ showed that the presence of an epoxy group next to a hydroxyl is more stable than two neighboring epoxy groups in GO, the stabilization is from the hydrogen bond between epoxy and hydroxyl, which from our experience it would not have direct influence on the anchoring of metal atoms or cluster, but might stabilize the whole system a bit more. However, to make our model to be simple we focus our investigation on the Pt atoms on a GO sheet that contains epoxy oxygen but no hydroxyl group or both.

On the GO ($C_{48}O_{16}$) sheet (Pt/GO), we used two Pt atoms to match the mass of composition of Pt (about 32 %), within a range of experimental observations in a common Pt/GO hybrid synthesis;^{13,14} we discuss in detail the adsorption behavior of methane and the reaction mechanisms.

2. Computational Details

We employed density-functional theory (DFT) and the plane-wave method, as implemented in the Vienna ab initio simulation package (VASP)¹⁹⁻²², to calculate the energies and structures of reactants, intermediates, transition structures and products of the reactions. We used the projector-augmented-wave method (PAW)²³⁻²⁴ in conjunction with the generalized gradient-approximation (GGA) and Perdew-Wang 1991(PW91) exchange-correlation function.

Experimental observations¹⁴ show that increased O/C ratios of GO sheets enhance the tolerance to CO poisoning of the metallic catalyst; the best condition was a GO sheet with O/C ratio 0.35. We thus selected a GO sheet that is composed of 48 carbon and 16 oxygen atoms (O/C = 0.33) to approach the experimental conditions. As shown in Fig. 1, the structure of a GO sheet with O/C ratio 0.33 consists of 16 epoxy groups and 8 unsaturated C=C double bonds in a parallelogram supercell with lattice parameters $a = 10.07$ and $b = 15.07$ Å; half the epoxy groups are on one side of the GO sheet and the other half on the opposite side.

The Monkhorst-Pack mesh k -point²⁵ ($5 \times 5 \times 1$) was used for surface calculations with energy truncated at 400 eV. The adsorption energies were calculated based on this equation,

$$E_{\text{ads}} = E_{\text{slab} + \text{adsorbate}} - (E_{\text{slab}} + E_{\text{adsorbate}}) \quad (1)$$

in which $E_{\text{slab} + \text{adsorbate}}$, E_{slab} , and $E_{\text{adsorbate}}$ are the calculated electronic energies of adsorbed species on the above surfaces and clean surfaces and for free molecules, respectively. We applied frequency calculations to verify the adsorbed intermediates and the transition states. The climbing-image nudged-elastic-band (CI-NEB) method²⁶⁻²⁸ was employed to locate the transition structures; paths of minimum energy (MEP) were constructed accordingly.

3. Results and discussion

3.1. Adsorption of platinum atoms on a GO sheet

In the top view of the graphene oxide with epoxy groups and O/C ratio = 0.33 and the diagram for the electronic-localization function (ELF)²⁹⁻³¹ shown in Fig. 1, we classify the components of the GO sheet into three major adsorption sites: (i) epoxy sites (onto the top site of O atoms: $O_{(a)}$, $O_{(b)}$, $O_{(c)}$, $O_{(d)}$), (ii) C=C sites (hollow of triangular shape formed by $O_{(a)}$, $O_{(b)}$, $O_{(c)}$), and (iii) C-C sites with an epoxy group underneath (hollow of triangular shape formed by $O_{(b)}$, $O_{(c)}$, $O_{(d)}$). Accordingly, we anchored a Pt atom on these regions of a GO sheet and found that the Pt atom was favorably adsorbed in the area surrounded by $O_{(a)}$, $O_{(b)}$, $O_{(c)}$ (C=C sites), at which it exhibited a greater value of the electronic localization function in Fig. 1(B) with adsorption energy -2.36 eV (a local minimum; no epoxy group is displaced (Fig. 2(a)); crossing an energy barrier of height 0.44 eV, the adsorbed Pt atom interacts with

ambient epoxy groups to achieve C–O–Pt bonding ($O_{(b)}$, $O_{(c)}$ and Pt atoms are slightly displaced) on the GO sheet with calculated larger adsorption energy -3.03 eV (a more favorable geometry for Pt/GO). The difference between these two structures, shown in Fig. 2(a) and (b), is that the former has less charge transferred from the Pt atom into the GO sheet through the carbon layer ($-0.26 |e|$ from a Bader charge calculation^{32,33}), but greater charge transfer for the latter ($-0.85 |e|$) via the epoxy groups ($O_{(b)}$ and $O_{(c)}$), accompanying the larger adsorption energy.

To assess the interaction between Pt atoms in our calculation, we employed also a model involving two Pt atoms on a GO sheet. The single Pt atom on a GO sheet (Pt/GO in Fig. 2(b)) would serve as a slab to anchor the second Pt atom, which was expected to be adsorbed at adjacent sites ((α) , (β) , and (γ) with a greater electronic localization function as calculated and shown in Fig. 1, to form Fig. 2(c), 2(d) and 2(e), respectively). The largest co-adsorption energy, -5.98 eV, in Fig. 2(c) indicated that $Pt_{(1)}$ and $Pt_{(2)}$ prefer to aggregate (the length of the $Pt_{(1)}$ – $Pt_{(2)}$ bond is 2.51 \AA), instead of being dispersed (the distance from $Pt_{(1)}$ to $Pt_{(2)}$ is 3.76 \AA in Fig 2(d)). Another Pt_2 aggregate structure (Fig. 2(e)) could have a co-adsorption energy -5.05 eV, which is also less than -5.98 eV in Fig. 2(c). Accordingly, we chose the structure of Fig. 2(c) with the largest co-adsorption energy as our calculated model of the Pt_2 /GO sheet for the subsequent calculations.

3.2. Adsorption and reaction of CH₄ on Pt₂/GO, Pt₂O₂/GO and Pt₂O/GO sheets

To investigate the CH₄ anchoring behavior on the Pt₂/GO sheet, we considered several adsorption modes of CH₄ around Pt₍₁₎ and Pt₍₂₎; we found that the most stable structure in our calculation is **IM-1** (shown in Fig. 3), in which the adsorbed CH₄ is located about Pt₍₂₎ with the calculated greatest adsorption energy, -0.53 eV, but the adsorption energies decrease to -0.11~ -0.30 eV on moving CH₄ about the Pt₍₁₎ atom that has a larger coordination number (Pt₍₁₎ already bonded to O_(b) and O_(c) atoms). The C-H bond of CH₄ in **IM-1** became elongated to 1.16Å (1.10Å in a free molecule) via the activation of Pt₍₂₎; the dehydrogenation of CH₄ required only 0.33 eV to overcome the energy barrier to form **IM-2**, CH₃-Pt₍₂₎ + H-Pt₍₂₎ (slightly endothermic, 0.06 eV); the absorbed H atom on Pt₍₂₎ might subsequently transfer toward the O_(c) atom to form **IM-3**, CH₃-Pt₍₂₎+ HO-Pt₍₁₎, with an energy barrier of height 0.80 eV and exothermicity 1.24 eV. Intermediate **IM3** might further dehydrogenate on crossing an energy barrier of height 0.92eV to produce a CH₂ species plus a water molecule (red line, **IM-3** → **IM-4**), or proceed to the CH₃ + OH combination (black line, **IM-3** → **IM-5**) on passing a much greater energy barrier, 1.76eV, to form CH₃OH_(a), which requires 1.39 eV to become desorbed from the sheet. According to the potential-energy diagram in Fig. 3, to produce CH₃OH without an extra added oxygen

atom, the adsorbed methane would react with the oxygen atom from the GO sheet (destroying the GO structure) at the expense of a much greater energy barrier.

We therefore simulated the adsorption of an O_2 molecule on a Pt_2/GO sheet, before methane joined the system, possibly to favor the conversion of methane to methanol. Figure 4 shows the optimized structures and a potential-energy profile for the methane conversion on a Pt_2O_2/GO sheet; the O_2 molecule lies horizontally on the Pt atoms to form Pt_2O_2 on a GO sheet with calculated adsorption energy -0.89 eV. The participation of two oxygen atoms increases the coordination number of the Pt_2 structure and thus the adsorption energy of CH_4 on the Pt_2O_2/GO sheet (around the $Pt_{(2)}$ atom) becomes slightly decreased to -0.34 eV (from -0.53 eV in Pt_2/GO); the elongated C–H bond (1.15 Å in **IM-6**) indicates, however, that the Pt atom retains its ability to activate the C–H bond. We considered several reaction orientations for the dehydrogenation of methane on a Pt_2O_2/GO sheet; the optimum path in our calculation is for the dissociated H atom to migrate to $O_{(e)}$ while the methyl group shifts to $Pt_{(2)}$ on passing an energy barrier 0.72 eV (**IM-6** \rightarrow **IM-7**). The formation of methanol via the CH_3-OH combination had to overcome energy barrier 0.71 eV to form an adsorbed methanol and a residual adsorbed oxygen atom on the Pt_2O/GO sheet (**IM-7** \rightarrow **IM-8**).

A second CH₄ was added onto the Pt₂O/GO sheet; the potential-energy profile diagram and optimized geometries appear in Fig 5. This adsorbed CH₄ also prefers to locate about the Pt₍₂₎ atom (**IM-9**), with adsorption energy -0.43 eV, and an extended C–H bond length, 1.17\AA . The C-H scission would induce the product CH₃-Pt₍₂₎ + HO_(f), with energy barrier 0.84 eV (**IM-9** → **IM-10**). The formation of methanol occurs through the combination of CH₃ and OH groups on crossing the energy barrier 1.03 eV, which can desorb with desorption energy 1.01 eV, so to recover the Pt₂/GO sheet, resulting in a net reaction $2\text{CH}_4 + \text{O}_2 \xrightarrow{[\text{Pt}_2/\text{GO}]} 2\text{CH}_3\text{OH}$.

In our calculation, the mechanism for methane → methanol was divided into three steps: (i) CH₄ activation, (ii) CH₄ + [MO] → CH₃-[M]-OH, and (iii) CH₃-[M]-OH → CH₃OH + [M]. Comparing the adsorption of CH₄ on Pt₂/GO, Pt₂O/GO and Pt₂O₂/GO sheets, we found that the adsorption energy was slightly decreased (-0.53 , -0.43 and -0.34 eV, respectively), but not the elongation of the C-H bond of methane ($d(\text{C-H}) = 1.16$, 1.15 and 1.17\AA , respectively), indicating that CH₄ activation was almost unaffected on increasing the oxygen atoms in the system. In the second step, CH₄ + [MO] → CH₃-[M]-OH, in which one oxygen atom of [MO] (from an epoxy group (O_c), the first (O_e), and second oxygen (O_f) from an added O₂ molecule, in Pt₂/GO, Pt₂O/GO, and Pt₂O₂/GO sheets, respectively) becomes reduced to OH, with similar energy barriers 0.80 , 0.84 and 0.72 eV, respectively, to form

CH₃-[M]-OH intermediates, IM-3 (Fig. 3), IM-7 (Fig. 4), and IM-10 (Fig. 5). The third step, a combination of CH₃ and OH groups to form CH₃OH, has distinct and decreased energy barriers 1.76, 1.03, and 0.71 eV, respectively, for Pt₂/GO, Pt₂O/GO, and Pt₂O₂/GO sheets. In this step, the CH₃ group might struggle from the constraint of Pt atoms to combine with the OH group, indicating that the energy barriers depended on the binding ability of the Pt atom with the CH₃ group, consistent with the oxidative degree of the catalyst (Pt₂/GO < Pt₂O/GO < Pt₂O₂/GO); the oxidative degree is inversely proportional to the binding ability of the Pt atom to the CH₃ group.

3.3. Comparison of adsorption behavior involving the Pt₂/GO sheet and a Pt cluster

As a support for catalytic materials, a GO sheet proved to be a great platform to make the Pt particles become dispersed,¹⁴ but the role of the GO sheet in the catalytic reaction on Pt/GO hybrid catalysts is little discussed. A low-symmetry isomer of the Pt₁₃ cluster was selected as a contrast to the Pt atoms on GO sheets (Pt₂/GO). From calculated data in Table 1, the Pt₁₃ cluster has a much larger energy for the adsorption of O₂ than Pt₂/GO (-1.68 vs. -0.89 eV), whereas it is almost inert to the CH₄ molecule relative to Pt₂/GO (-0.06 vs. -0.53 eV). We have calculated the partial density of states (*p*DOS) projected onto the total d-band (blue line) shown

in Fig. 6, with the d_z^2 state (purple line) of $Pt_{(1)}$ and $Pt_{(2)}$ on Pt_2/GO and Pt_{13} cluster ($Pt_{(1)}$ and $Pt_{(2)}$ were the most active atoms of Pt_{13} cluster); the red lines in 6b and 6d represent the p-state of adsorbed O_2 ($O_{(1)}$ and $O_{(2)}$). The d-band structures of Pt on Pt_2/GO and O_2-Pt_2/GO (Fig. 6a and 6b) display a specific band structure about +2 ~ +4 eV (unique from Fig. 6c and 6d) that is completely contributed from the d_z^2 state, indicating that this band structure is strongly related to the existence of the GO sheet: it hence arises from a hybrid of Pt atoms and the GO sheet.

We focus on this specific band area of the d_z^2 state of Pt atoms on a GO sheet before and after the adsorption of CH_4 , shown in Fig. 7. After adsorption, the original d_z^2 state attained about +2 ~ +4 eV shifted to ca. -6 ~ -7 eV and generated an evident area of overlap with the hydrogen s orbital of a C-H bond; this result clearly demonstrates that the split d_z^2 state above the Fermi level plays an important role in the activation of the C-H bond of a CH_4 molecule. We observed also a similar split d_z^2 state that appeared on the Pt_2O_2/GO sheet (Fig. 6b), consistent with the fact that the Pt atoms on the Pt_2O_2/GO sheet exhibit an ability to activate the C-H bond of methane ($E_{ad} = -0.34$ eV, and $d(C-H) = 1.15$ Å as shown in Table 1). The specific d_z^2 band above the Fermi level showed a strong adsorption for the CH_4 molecule on the $IrO_2(110)$ surface with a small energy barrier for the first hydrogen abstraction.³⁴ In summary, we found that the GO sheet split the d-band structure and generate some d_z^2

band above the Fermi level of the Pt atoms, which enhances an activation of the C-H bond of a CH₄ molecule.

4. Conclusion

In this work, we used two Pt atoms loaded onto a GO sheet (C₄₈O₁₆) to match the mass of composition of Pt (about 32 %) within the range of experimental observation in a common Pt/GO hybrid synthesis (about 30 %).^{13, 14} From our calculation of the density of states, we found a specific d-band structure about +2 ~ +4 eV, contributed solely from the d_{z²} state of Pt on the GO sheet, which enables activation of a C-H bond of CH₄ and simultaneously shifted the band to -6 ~ -7 eV; a moderate energy of adsorption of CH₄ on the Pt/GO system is exhibited, relative to pure Pt cluster counterparts that are almost inert to a CH₄ molecule. The addition of a dioxygen molecule enables a reaction with activated CH₄, according to mechanisms for 2 CH₄ + O₂ $\xrightarrow{[Pt_2/GO]}$ 2 CH₃OH, so that the Pt₂/GO system becomes a potential catalyst for the production of methanol through adding methane and O₂ to the system.

Acknowledgements

Ministry of Science and Technology of Republic of China (NSC 102-2113-M-003-008-MY4) supported this work; National Center for High-performance Computing provided computer time and facilities.

References

- 1 J. Milewski, A. Miller and J. Sałacinski, *Int. J. Hydrogen Energy*, 2007, **32**, 687–698.
- 2 N. R. Peela, J. E. Sutton, I. C. Lee, and D. G. Vlachos, *Ind. Eng. Chem. Res.*, 2014, **53**, 10051–10058.
- 3 Y. Chen and D. G. Vlachos, *Ind. Eng. Chem. Res.*, 2012, **51**, 12244–12252.
- 4 A. B. Mhadeshwar and D. G. Vlachos, *J. Phys. Chem. B*, 2005, **109**, 16819–16835.
- 5 G. Psfogiannakis, A. S. Amant and M. Ternan, *J. Phys. Chem. B*, 2006, **110**, 24593–24605.
- 6 L. C. Jacobson and V. Molinero, *J. Phys. Chem. B*, 2010, **114**, 7302–7311.
- 7 J. Wei and E. Iglesia, *J. Phys. Chem. B*, 2004, **108**, 4094–4103.
- 8 V. Havran, M. P. Dudukovi'c and C. S. Lo, *Ind. Eng. Chem. Res.*, 2011, **50**, 7089–7100.
- 9 A. Dianat, N. Seriani, L. C. Ciacchi, W. Pompe, G. Cuniberti and B. Bobeth, *J. Phys. Chem. C*, 2009, **113**, 21097–21105.
- 10 J. Chen, B. Lim, E. P. Lee and Y. Xia, *Nano Today*, 2009, **4**, 81–95.
- 11 M. Yang, M. Zhou, A. Zhang and C. Zhang, *J. Phys. Chem. C*, 2012, **116**, 22336–22340.

- 12 I. Fampiou and A. Ramasubramaniam, *J. Phys. Chem. C*, 2013, **117**, 19927–19933.
- 13 A. Grinou, Y. S. Yun, S. Y. Cho, H. H. Park and H.-J. Jin, *Materials*, 2012, **5**, 2927–2936.
- 14 S. Sharma, A. Ganguly, P. Papakonstantinou, X. Miao, M. Li, J. L. Hutchison, M. Delichatsios and S. Ukleja, *J. Phys. Chem. C*, 2010, **114**, 19459–19466.
- 15 S.Y. Wu and J.J. Ho. *J. Phys. Chem.C*, 2014, **118**, 26764-26771.
- 16 G. Kim and S.-H. Jhi, *ACS Nano*, 2011, **5 (2)**, pp 805–810.
- 17 L. Wang, Y. Y. Sun, K. Lee, D. West, Z. F. Chen, J. J. Zhao and S. B. Zhang, *Phys. Rev. B*, 2010, **82**, 161406–161409(R).
- 18 D. W. Boukhvalov and M. I. Katsnelson, *J. Am. Chem. Soc.*, 2008, **130**, 10697–10701.
- 19 G. Kresse and J. Hafner, *Phys. Rev. B*, 1993, **47**, 558–561.
- 20 G. Kresse and J. Hafner, *Phys. Rev. B*, 1994,**49**, 14251–14269.
- 21 G. Kresse and J. Furthmuller, *Comp. Mater. Sci.*, 1996, **6**, 15–50.
- 22 G. Kresse and J. Hafner, *Phys. Rev. B*, 1996, **54**, 11169–11186.
- 23 P. E. Blöchl, *Phys. Rev. B*, 1994, **50**, 17953–17979.
- 24 G. Kresse and D. Joubert, *Phys. Rev. B*, 1999, **59**, 1758–1775.
- 25 H. J. Monkhorst and J. D. Pack, *Phys. Rev. B*, 1976,**13**, 5188–5192.

- 26 G. Henkelman, B. P. Uberuaga and H. Jónsson, *J. Chem. Phys.*, 2000, **113**, 9901–9904.
- 27 D. Sheppard and G. Henkelman, *J. Comp. Chem.*, 2011, **32**, 1769–1771.
- 28 D. Sheppard, R. Terrell and G. Henkelman, *J. Chem. Phys.*, 2008, **128**, 134106–1–10.
- 29 B. Silvi and A. Savin, *Nature*, 1994, **371**, 683–686.
- 30 A. Savin, A. D. Becke, J. Flad, R. Nesper, H. Preuss and H. G. von Schnering, *Angew. Chem. Int. Ed. Engl.*, 1991, **30**, 409–412.
- 31 A. D. Becke and K. E. Edgecombe, *J. Chem. Phys.*, 1990, **92**, 5397–5403.
- 32 R. F. W. Bader, *Chem. Rev.*, 1991, **91**, 893–928.
- 33 G. Henkelman, A. Arnaldsson and H. Jónsson, *Comput. Mater. Sci.*, 2006, **36**, 254–360.
- 34 C.-C. Wang, S. S. Siao and J.-C. Jiang, *J. Phys. Chem. C*, 2012, **116**, 6367–6370.

Table 1. (a) Adsorption energy/eV and selected geometric parameters of O₂ adsorption on Pt₂/GO sheet and Pt₁₃ cluster, (b) electronic structures of Pt₍₁₎ and Pt₍₂₎ before and after adsorption of O₂, and (c) adsorption energy/eV and selected geometric parameters of O₂ adsorption on Pt₂-GO, O₂-Pt₂/GO, Pt₁₃ and O₂-Pt₁₃ cluster.

(a) O ₂ adsorption				
	Pt ₂ /GO		Pt ₁₃ cluster	
$E_{\text{ads}}(\text{O}_2)/\text{eV}$	-0.89		-1.68	
$d(\text{O}-\text{O})/\text{\AA}$	1.39		1.41	
$q(\text{e}^-)$ of O _{2(a)}	-0.56		-0.72	
(b) electronic structures (sum of Pt ₍₁₎ and Pt ₍₂₎)				
	Pt ₂ /GO	Pt ₂ O ₂ /GO	Pt ₁₃ cluster	O ₂ -Pt ₁₃ cluster
ϵ_{d} of Pt/eV	-2.17	-2.34	-2.04	-3.18
$q(\text{e}^-)$ of Pt	+1.04	+1.61	-0.18	+0.82
(c) CH ₄ adsorption				
	Pt ₂ -GO	Pt ₂ O ₂ /GO	Pt ₁₃ cluster	O ₂ -Pt ₁₃ cluster
$E_{\text{ads}}(\text{CH}_4)/\text{eV}$	-0.53	-0.34	-0.06	-0.08
$d(\text{C}-\text{H})/\text{\AA}$	1.16	1.15	1.10	1.10

* Pt₍₁₎ and Pt₍₂₎ are marked in Fig. 6.

Figure

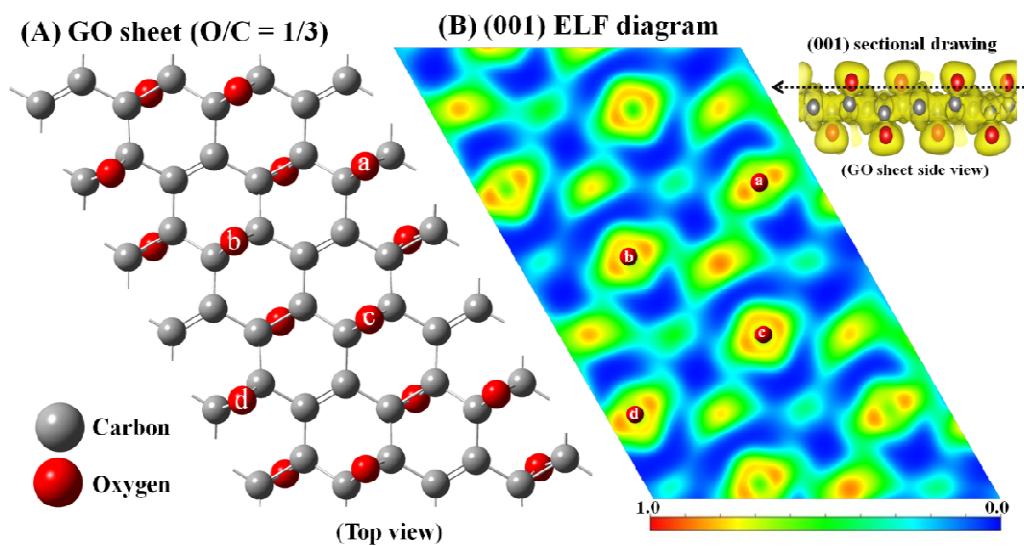


Figure 1. (a) Top view of an optimized GO sheet with O/C ratio 0.33, consisting of 16 epoxy groups and 8 unsaturated C=C double bonds. (b) Top view of the electron-localization function (ELF) diagram of the GO sheet.

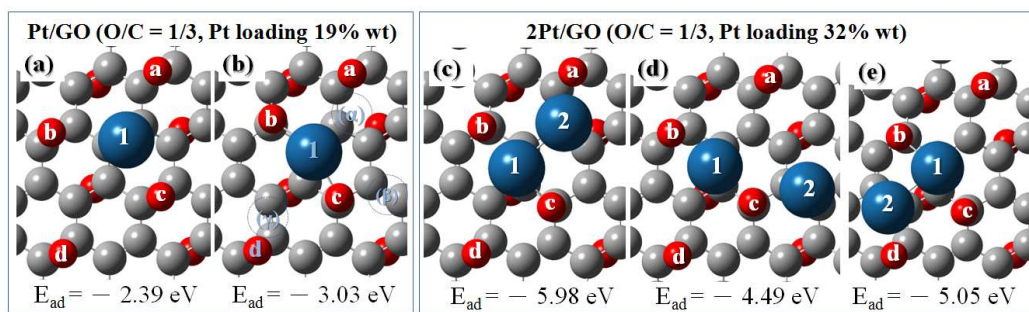


Figure. 2. Top view of optimized structures of anchored platinum atoms on a GO sheet ($O/C = 1/3$) at various positions.

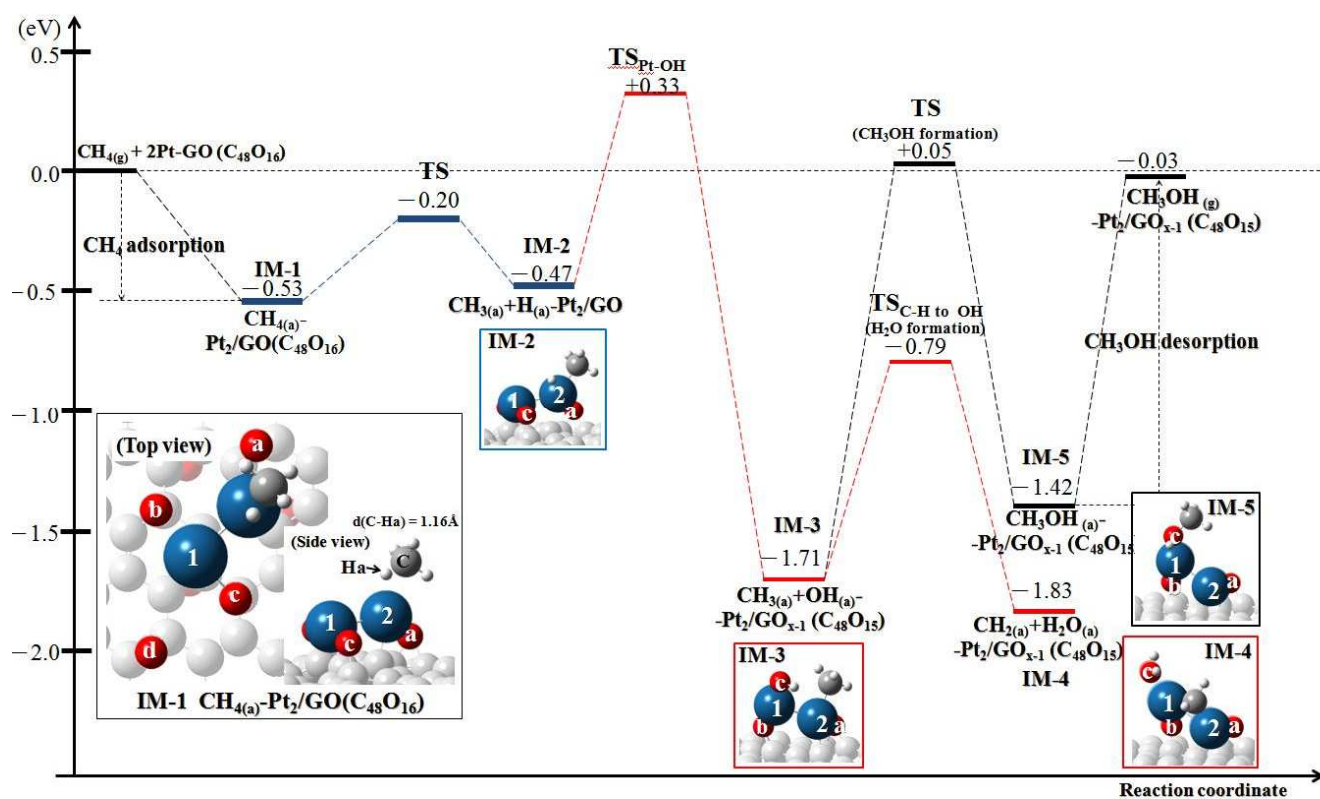


Figure 3. Calculated potential-energy diagram of methane conversion on a Pt₂/GO sheet, with optimized geometries of various intermediates, including the top and side views of IM-1, and side views of IM-2 to IM-5.

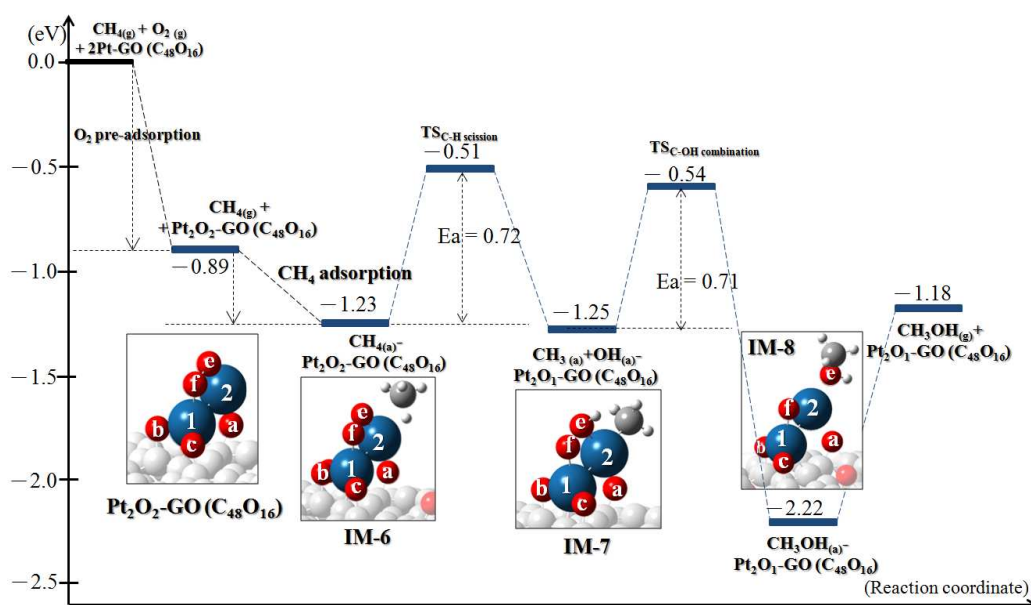


Figure 4. Calculated optimum potential-energy diagram of methane conversion on a Pt₂O₂/GO sheet, with optimized geometries of various intermediates.

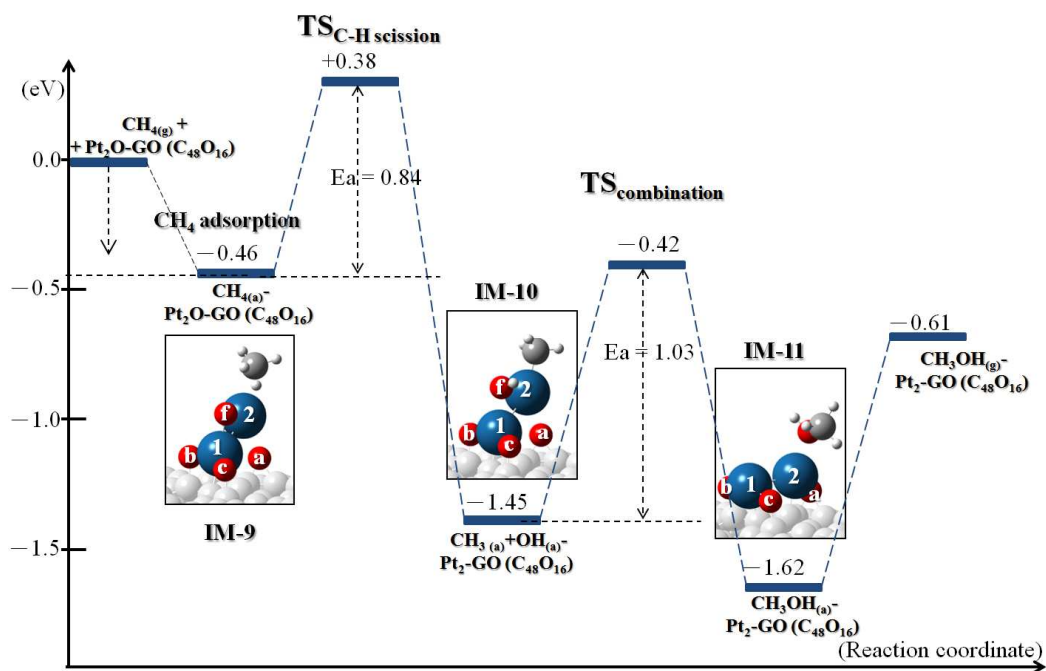


Figure 5. Calculated optimum potential-energy diagram of methane conversion on a Pt₂O/GO sheet, with optimized geometries of various intermediates.

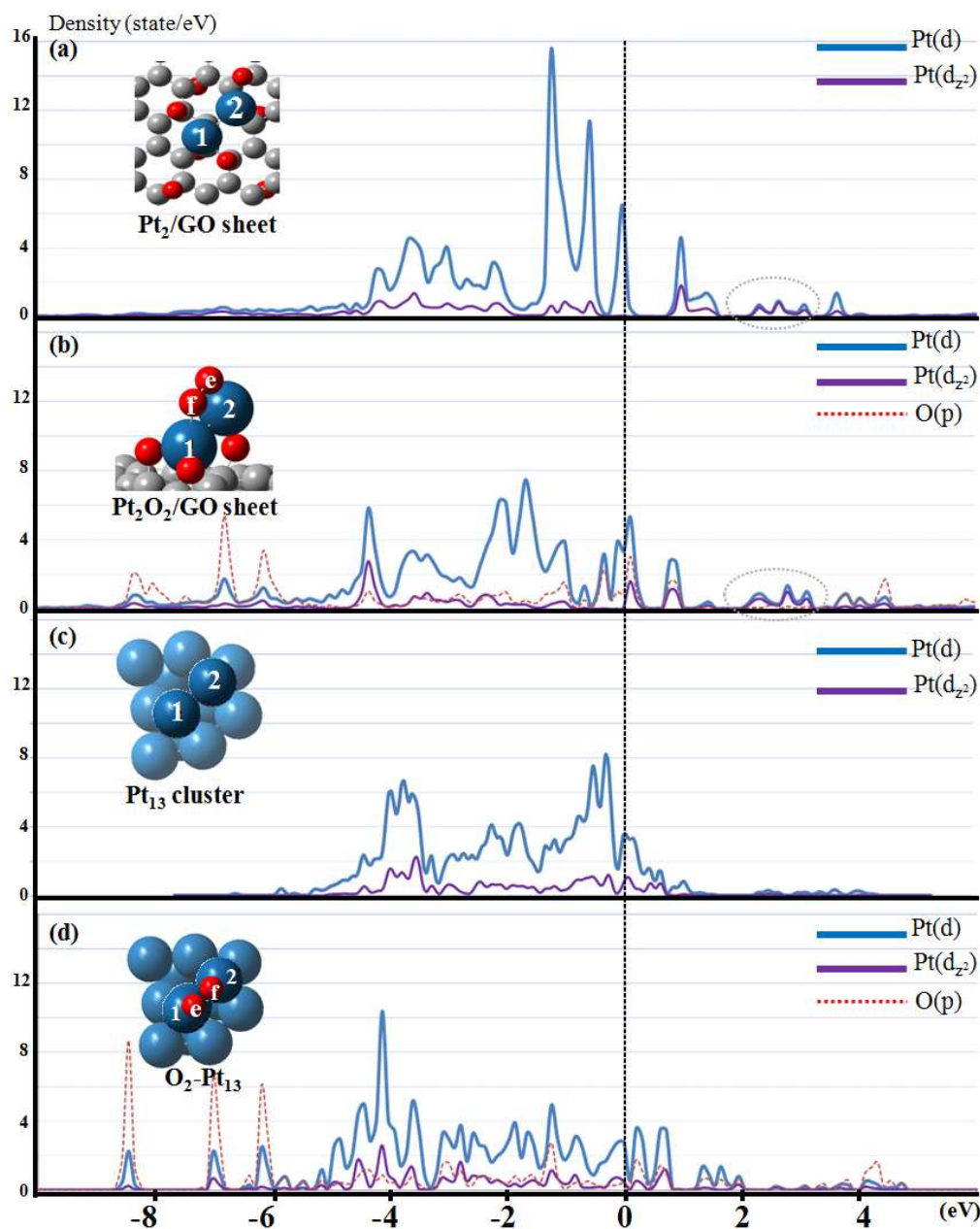


Figure 6. Partial density of states (*pDOS*) projected onto the total d-band (blue line) and d_z^2 state (purple line) of Pt₍₁₎ and Pt₍₂₎ on Pt₂/GO and a Pt₁₃ cluster, respectively; the red lines in 6b and 6d represent the p-state of the adsorbed O₂ (O₍₁₎ and O₍₂₎).

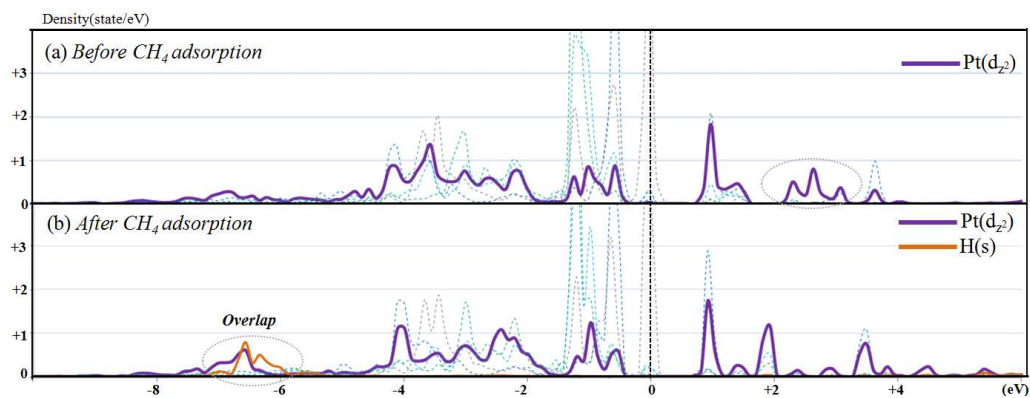
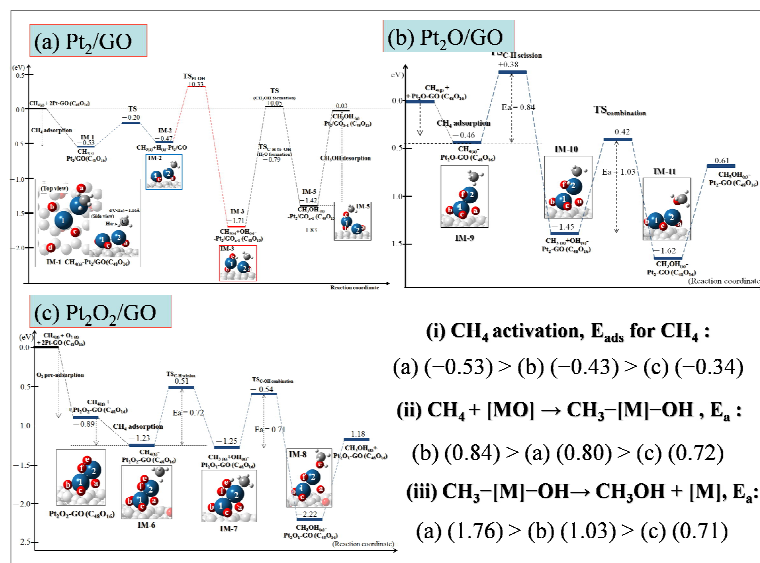


Figure. 7 p DOS in the d_z^2 state (purple line) of Pt atoms on a GO sheet before and after adsorption of CH_4 . The dashed lines represent four d-states other than d_z^2 ; an orange line in Fig. 7b represents the s orbital of a hydrogen of CH_4 adsorbed on the Pt_2/GO sheet.

Table of Contents Graphic



Calculated optimum potential-energy diagram of methane conversion on (a) Pt₂/GO (b) Pt₂O/GO, (c) Pt₂O₂/GO sheets.